Inhaled seralutinib exhibits potent efficacy in models of pulmonary arterial hypertension

Anna Galkin[1,5], Ravikumar Sitapara[1,2,5], Bryan Clemons[1], Eduardo Garcia[1], Michael Kennedy[1], David Guimond[1], Laura L. Carter[1], Ashley Douthitt ⓘ[1], Robin Osterhout[1], Aneta Gandjeva[3], Deborah Slee[1], Luisa Salter-Cid[1], Rubin M. Tuder[3] and Lawrence S. Zisman[1,4]

[1]Gossamer Bio, Inc., San Diego, CA, USA. [2]The Rensselaer Center for Translational Research Inc., Rensselaer, NY, USA. [3]University of Colorado School of Medicine, Aurora, CO, USA. [4]Pulmokine Inc., Troy, NY, USA. [5]A. Galkin and R. Sitapara contributed equally as first authors.

Corresponding author: Lawrence S. Zisman (lzisman@gossamerbio.com)

Abstract

Background Signalling through platelet-derived growth factor receptor (PDGFR), colony-stimulating factor 1 receptor (CSF1R) and mast/stem cell growth factor receptor kit (c-KIT) plays a critical role in pulmonary arterial hypertension (PAH). We examined the preclinical efficacy of inhaled seralutinib, a unique small-molecule PDGFR/CSF1R/c-KIT kinase inhibitor in clinical development for PAH, in comparison to a proof-of-concept kinase inhibitor, imatinib.

Methods Seralutinib and imatinib potency and selectivity were compared. Inhaled seralutinib pharmacokinetics/pharmacodynamics were studied in healthy rats. Efficacy was evaluated in two rat models of PAH: SU5416/Hypoxia (SU5416/H) and monocrotaline pneumonectomy (MCTPN). Effects on inflammatory/cytokine signalling were examined. PDGFR, CSF1R and c-KIT immunohistochemistry in rat and human PAH lung samples and microRNA (miRNA) analysis in the SU5416/H model were performed.

Results Seralutinib potently inhibited PDGFRα/β, CSF1R and c-KIT. Inhaled seralutinib demonstrated dose-dependent inhibition of lung PDGFR and c-KIT signalling and increased bone morphogenetic protein receptor type 2 (BMPR2). Seralutinib improved cardiopulmonary haemodynamic parameters and reduced small pulmonary artery muscularisation and right ventricle hypertrophy in both models. In the SU5416/H model, seralutinib improved cardiopulmonary haemodynamic parameters, restored lung BMPR2 protein levels and decreased N-terminal pro-brain natriuretic peptide (NT-proBNP), more than imatinib. Quantitative immunohistochemistry in human lung PAH samples demonstrated increased PDGFR, CSF1R and c-KIT. miRNA analysis revealed candidates that could mediate seralutinib effects on BMPR2.

Conclusions Inhaled seralutinib was an effective treatment of severe PAH in two animal models, with improved cardiopulmonary haemodynamic parameters, a reduction in NT-proBNP, reverse remodelling of pulmonary vascular pathology and improvement in inflammatory biomarkers. Seralutinib showed greater efficacy compared to imatinib in a preclinical study.

Introduction

Pulmonary arterial hypertension (PAH) is characterised by perivascular inflammation and proliferation of pulmonary artery smooth muscle cells (PASMCs), myofibroblasts and endothelial cells, resulting in pulmonary arterial blood flow obstruction [1–6]. The emergence of apoptosis-resistant cells within pulmonary vascular lesions led to the cancer paradigm hypothesis to explain the abnormal cell proliferation observed in PAH lesions [1, 4, 5, 7, 8].

Within the context of this cancer-like paradigm, evidence from human PAH lung explants, cell-based assays and preclinical models points to a pivotal role of platelet-derived growth factor (PDGF) signalling in PAH pathogenesis [9–14]. Expression of PDGF ligands and receptors (PDGF receptors α and β (PDGFRα/β)) was increased in small pulmonary arteries of patients with idiopathic PAH (iPAH) *versus* controls, and *PDGFB* gene expression was increased in a single-cell RNA sequencing study in iPAH [11, 15]. Genetic knockout studies suggest that PDGFRα and PDGFRβ mediate overlapping and distinct effects across PAH-associated pathways: both receptors regulate cell proliferation, migration and inflammation, while PDGFRβ may uniquely affect angiogenesis [16]. Crosstalk between PDGFR and other signalling cascades implicated in PAH, such as transforming growth factor β (TGF-β), has been reported [17, 18]. Furthermore, PDGF signalling decreased bone morphogenetic protein receptor type 2 (BMPR2) expression in PASMCs *via* miRNA-376b-mediated degradation [9]. These findings highlight the therapeutic potential of PDGFR kinase inhibitors for iPAH [19].

Imatinib (a potent PDGFR/ABL/c-KIT kinase inhibitor) reversed pulmonary hypertension in the rat monocrotaline (MCT) model, demonstrating histological and functional improvements [12]. In clinical trials, imatinib improved pulmonary vascular resistance (PVR) and exercise capacity in patients with advanced PAH; however, serious adverse events and discontinuations were common, limiting its development as a PAH treatment [20, 21].

Given the robust evidence implicating PDGFR signalling in PAH pathogenesis and limitations associated with systemic administration of PDGFR inhibitors [21], seralutinib (N-[3-[(1S)-1-[[6-(3,4-dimethoxyphenyl) pyrazin-2-yl]amino]ethyl]phenyl]-5-methylpyridine-3-carboxamide, formerly PK10571 and also known as GB002) was designed and formulated as a dry powder for inhalation drug delivery. In addition to its potent inhibition of PDGFRα and PDGFRβ, seralutinib inhibits PDGFR-related kinases, colony-stimulating factor 1 receptor (CSF1R) and mast/stem cell growth factor receptor kit (c-KIT), which are implicated in PAH pathogenesis and progression [22–26]. c-KIT is expressed on endothelial progenitor cells and mast cells, potentially contributing to perivascular inflammation and vascular remodelling [8, 23, 27]. Increased infiltration of c-KIT^{+} cells has been observed in pulmonary arterial plexiform lesions in PAH patient lungs [23]. CSF1R is expressed on monocytes and macrophages [22]. Macrophages secrete PDGF ligands and pro-inflammatory cytokines contributing to pathological remodelling in PAH [24, 25, 28]. Thus, a compelling rationale exists to target PDGFR, CSF1R and c-KIT as a treatment for PAH. Seralutinib targets these pathways and is the first tyrosine kinase inhibitor in clinical development specifically designed as an inhalation therapy for PAH. Given the limitations of imatinib, seralutinib was intentionally developed with low oral bioavailability and rapid clearance characteristics to minimise systemic exposure and associated adverse events.

The objectives of the preclinical studies reported here were to investigate the *in vitro* potency and selectivity of seralutinib and characterise its efficacy as compared to imatinib in relevant animal models of PAH.

Methods

The potency and selectivity of seralutinib and imatinib were determined *in vitro*. Pharmacokinetic and pharmacodynamic effects of inhaled seralutinib were studied in healthy rats. Efficacy was evaluated in the rat SU5416/Hypoxia (SU5416/H) (Study 1 and 3) and MCT pneumonectomy (MCTPN) (Study 2) models. In Study 1, treatment was initiated 1 day after a 3-week hypoxia exposure; in Study 2, treatment was started on day 25 after pneumonectomy (day 15 after MCT administration). In Study 3, seralutinib or imatinib was started 2 weeks after return to normoxia, subsequent to the 3-week hypoxia period. Treatment effects on echocardiographic parameters, cardiopulmonary haemodynamic parameters, N-terminal pro-brain natriuretic peptide (NT-proBNP), BMPR2 and inflammatory markers were examined. PDGFR, CSF1R and c-KIT immunohistochemistry (IHC) was performed with rat and human lung PAH and control samples. microRNA (miRNA) analysis of SU5416/H lungs (Study 3) was performed. Detailed methods are available in the supplementary material.

Results

In vitro *activity of seralutinib*

Seralutinib inhibited proliferation of H1703 (a PDGFRα-driven human lung epithelial cell line), human pulmonary arterial smooth muscle cells (HPASMCs) (which express similar levels of PDGFRα and PDGFRβ) and human lung fibroblasts (HLFs) (which express PDGFRβ more than PDGFRα) with median inhibitory concentrations (IC_{50}s) of 32 nM, 33 nM and 29 nM, respectively (figure 1, supplementary table S1). Although imatinib inhibited H1703 proliferation with an IC_{50} of 62 nM, its potency was 13–20-fold less than seralutinib in human PASMC and HLF proliferation assays. Both compounds potently inhibited
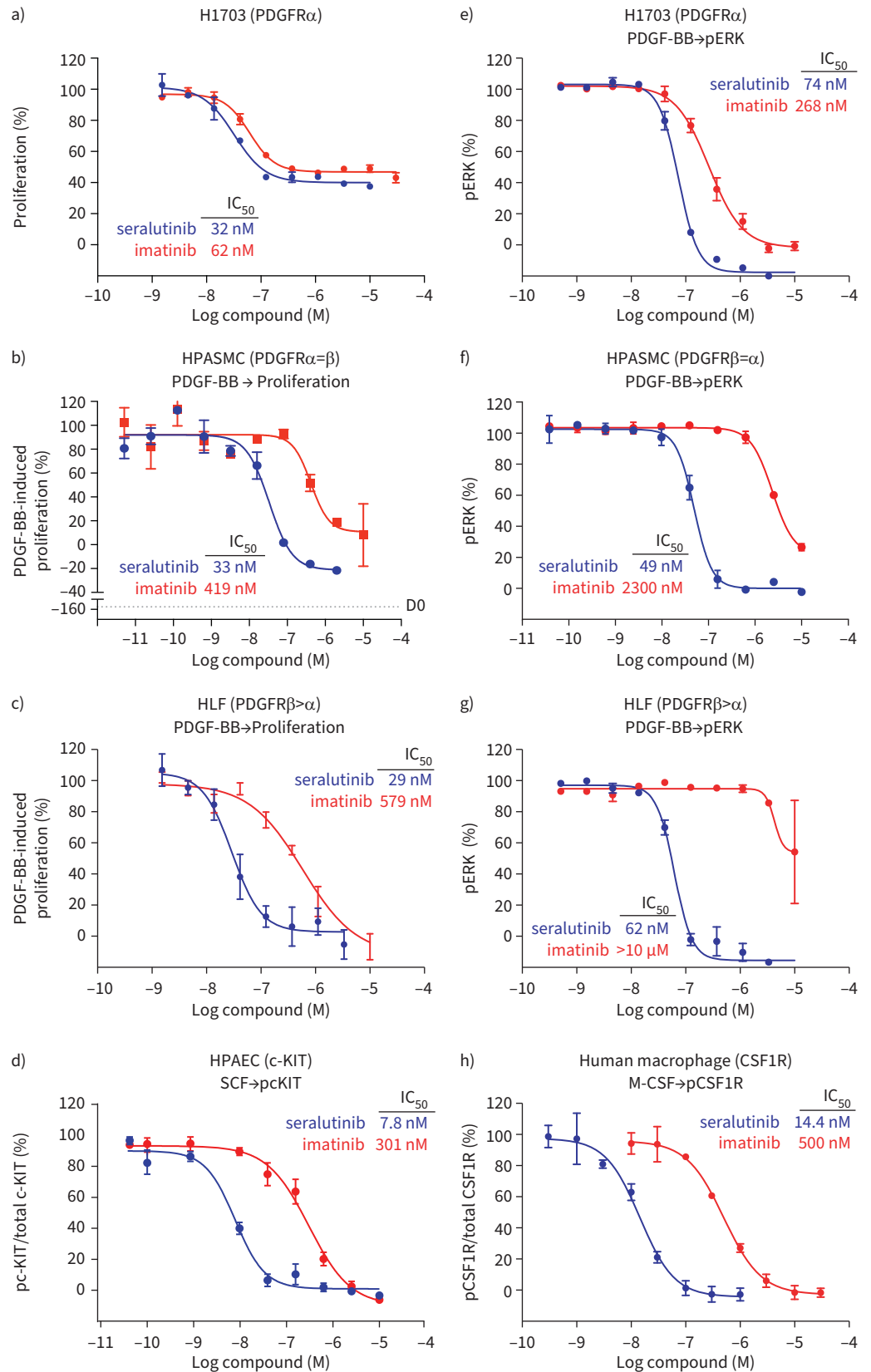
FIGURE 1 *In vitro* cell-based potency of seralutinib *versus* imatinib. Inhibition of proliferation in a) constitutively active platelet-derived growth factor receptor α (PDGFRα)-driven human lung epithelial cells (H1703), b) platelet-derived growth factor-BB (PDGF-BB) stimulated human pulmonary arterial smooth muscle

cells (HPASMCs) and c) human lung fibroblasts (HLFs) measured using CyQuant or CellTiter-Glo assays. For b) and c), the values for each concentration were normalised to 3 days of PDGF-BB stimulation (considered 100% proliferation) and no stimulation for 3 days (0% proliferation). For the HPASMC proliferation assay (b), D0 represents the basal value at day 0 prior to PDGF-BB stimulation. d) Inhibition of stem-cell factor (SCF)-induced phosphorylation of mast/stem cell growth factor receptor kit (c-KIT) in human pulmonary artery endothelial cells (HPAECs) (ELISA assay). Inhibition of PDGF-BB-induced phosphorylation of extracellular signal-regulated kinase in e) H1703, f) HPASMCs and g) HLFs was measured using a homogeneous time-resolved fluorescence (HTRF) assay. h) Macrophage colony-stimulating factor (M-CSF)-induced phosphorylation of colony-stimulating factor 1 receptor (CSF1R) in human primary macrophages (ELISA assay). Error bars represent the standard deviation of duplicate or triplicate measurements. Data are presented as the half maximal inhibitory concentration (IC_{50}) values (nM) for seralutinib (blue) and imatinib (red). pERK: phosphorylated ERK; pc-KIT: phosphorylated c-KIT.

PDGF-BB-induced extracellular signal-regulated kinase (ERK) phosphorylation in H1703 cells; however, only seralutinib inhibited ERK phosphorylation in HLFs (figure 1, supplementary table S1). Furthermore, seralutinib was more potent than imatinib against c-KIT and CSF1R kinases. Seralutinib inhibited stem-cell factor (SCF)-induced c-KIT autophosphorylation in human pulmonary artery endothelial cells (HPAECs) with an IC_{50} of 7.8 nM and displayed an IC_{50} of 14.4 nM in macrophage colony-stimulating factor (M-CSF)-induced phosphorylation of CSF1R in human primary differentiated macrophages (34-fold more potent than imatinib) (supplementary table S1, figure 1).

Pharmacokinetic and pharmacodynamic studies

Seralutinib lung concentration peaked immediately after a 2-h passive inhalation and steadily declined over time in rats. Substantially lower plasma exposures were observed relative to lung exposures (figure 2a). Four independent rat pharmacokinetic studies demonstrated an average seralutinib lung-to-plasma ratio of 30 (range 16–80) over a 24-h period. Seralutinib inhalation significantly inhibited PDGF-BB-induced PDGFRα/β autophosphorylation in the lung across all three dose levels tested (figure 2b, c). In a separate experiment, with co-administered intratracheal PDGF-BB and SCF, seralutinib inhibited c-KIT Y719 phosphorylation by 43% (figure 2d). Seralutinib inhibition of PDGFRβ phosphorylation in this experiment was similar to that observed when PDGF-BB was given alone. Furthermore, seralutinib demonstrated a 2-to-2.5-fold dose-dependent increase in lung BMPR2 protein expression over time (figure 2e).

Seralutinib efficacy in preclinical models of PAH

SU5416/H model (Study 1)

Two cohorts, with and without telemetry monitoring, received seralutinib 2.5 mg·kg^{-1} and 4.6 mg·kg^{-1} twice daily, respectively, for 2 weeks (figure 3a). Prior to initiating treatment, elevated pulmonary artery systolic pressure (PASP) was confirmed in vehicle (100.8±5 mmHg) and seralutinib (99.1±8 mmHg) groups by telemetry. Seralutinib 2.5 mg·kg^{-1} twice daily reduced PASP by 43% (p<0.0001) relative to vehicle at the end of treatment (figure 3b). End-of-study right ventricular systolic pressure (RVSP) measurements revealed a dose-dependent reduction with seralutinib compared to vehicle (2.5 mg·kg^{-1}: 49.6±3.1 mmHg *versus* 64.4±5.4 mmHg, p<0.05; 4.6 mg·kg^{-1}: 34.7±2.2 mmHg *versus* 64.4±5.4 mmHg, p<0.001) (figure 3c). A reduction in RV hypertrophy was observed in both seralutinib groups (2.5 mg·kg^{-1}: 0.36±0.01, p<0.0001; 4.6 mg·kg^{-1}: 0.40±0.02, p<0.005) compared to vehicle (0.54±0.03) (figure 3d).

Small pulmonary artery occlusion analysis (vessel diameter <80 µm) was performed in lung tissues from vehicle and seralutinib 4.6 mg·kg^{-1} twice daily groups. A significant decrease was observed in the number of grade 2 lesions in the seralutinib-treated group compared to vehicle (p<0.05; figure 3e, f). Small pulmonary artery lumen-to-media area was increased in the seralutinib-treated group compared to vehicle (p<0.05; figure 3g). IHC of lungs for phospho-PDGFRβ revealed reduced intensity in the seralutinib-treated group compared to vehicle (figure 3h).

MCTPN model (Study 2)

In the MCTPN model, seralutinib 2.5 mg·kg^{-1} twice daily was initiated after PAH development, and continued for 11 days (figure 4a). PASP remained stable in the seralutinib group but continued to increase in the vehicle group (figure 4b). On days 9, 10 and 11, PASP was 34%, 37% and 41% lower, respectively, in the seralutinib group compared to vehicle (p<0.05). A 50% reduction in RVSP was observed in the seralutinib group compared to vehicle (p<0.001; figure 4c). Right ventricular hypertrophy was reduced by 49% in the seralutinib group compared to vehicle (p<0.0001; figure 4d). Lumen-to-media area was increased in the seralutinib-treated group compared to controls, which indicates favourable reverse
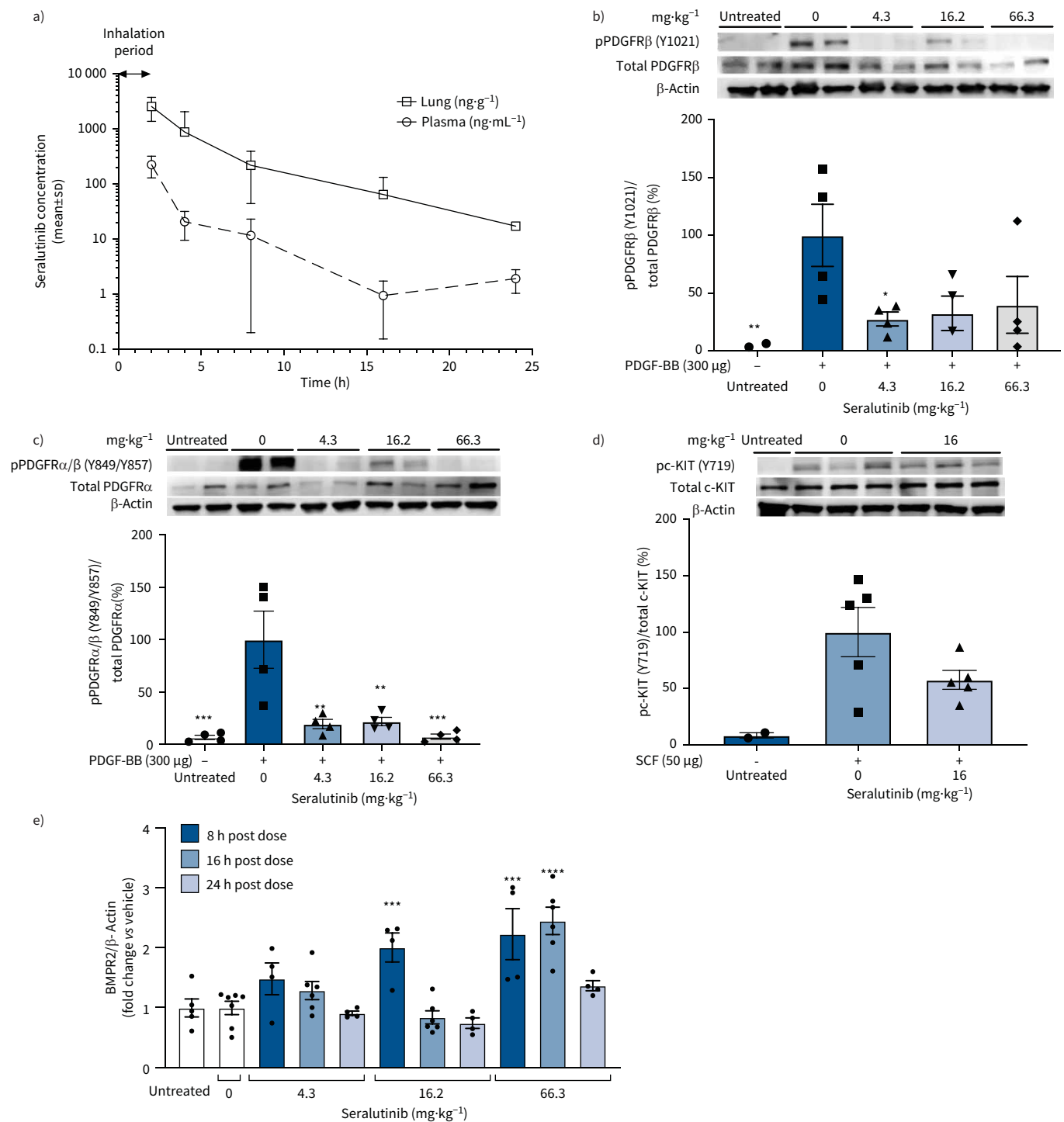
FIGURE 2 Seralutinib *in vivo* pharmacokinetic/pharmacodynamic profile. Male Sprague-Dawley rats received vehicle or seralutinib 4.3 mg·kg^{-1}, 16.2 mg·kg^{-1} and 66.3 mg·kg^{-1} *via* passive inhalation. a) Seralutinib concentrations in lung (square) and plasma (circle) over 24 h post 4.3 mg·kg^{-1} passive inhalation. For pharmacodynamic readout in lungs, rats were administered platelet-derived growth factor-BB (PDGF-BB) and stem-cell factor (SCF) *via* intratracheal insufflation into the lungs immediately post-dosing. 5 min post-challenge, lungs were harvested to measure phosphorylation of platelet-derived growth factor receptor (PDGFR) and mast/stem cell growth factor receptor kit (c-KIT). Data are presented as the per cent change in b) phosphorylated (p)PDGFRβ (Y1021)/total PDGFRβ, c) pPDGFRα/β (Y849/Y857)/PDGFRα and d) pc-KIT/total c-KIT in lung homogenates by Western blot analysis. e) Mean fold change in lung bone morphogenetic protein receptor type 2 (BMPR2)/β-Actin protein expression at 8, 16 and 24 h post-seralutinib dosing. Data are presented as mean±SEM (n=4 for a–c, n=2–5 for d, n=4–8 for e). Statistical analysis was performed using one-way ANOVA with Dunnett's multiple comparisons test. *: $p < 0.05$; **: $p < 0.005$; ***: $p < 0.001$; ****: $p < 0.0001$ seralutinib *versus* vehicle treatment group.
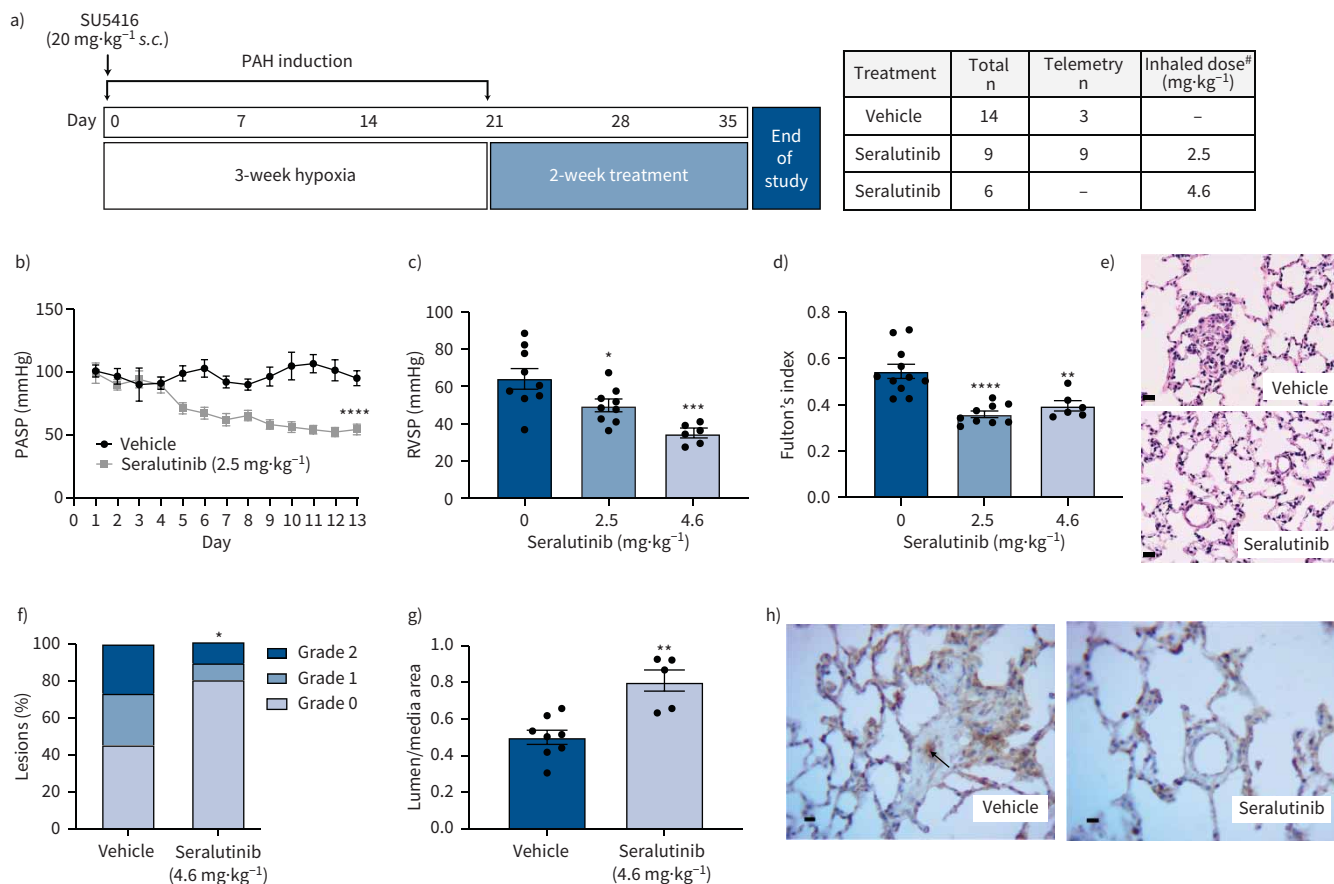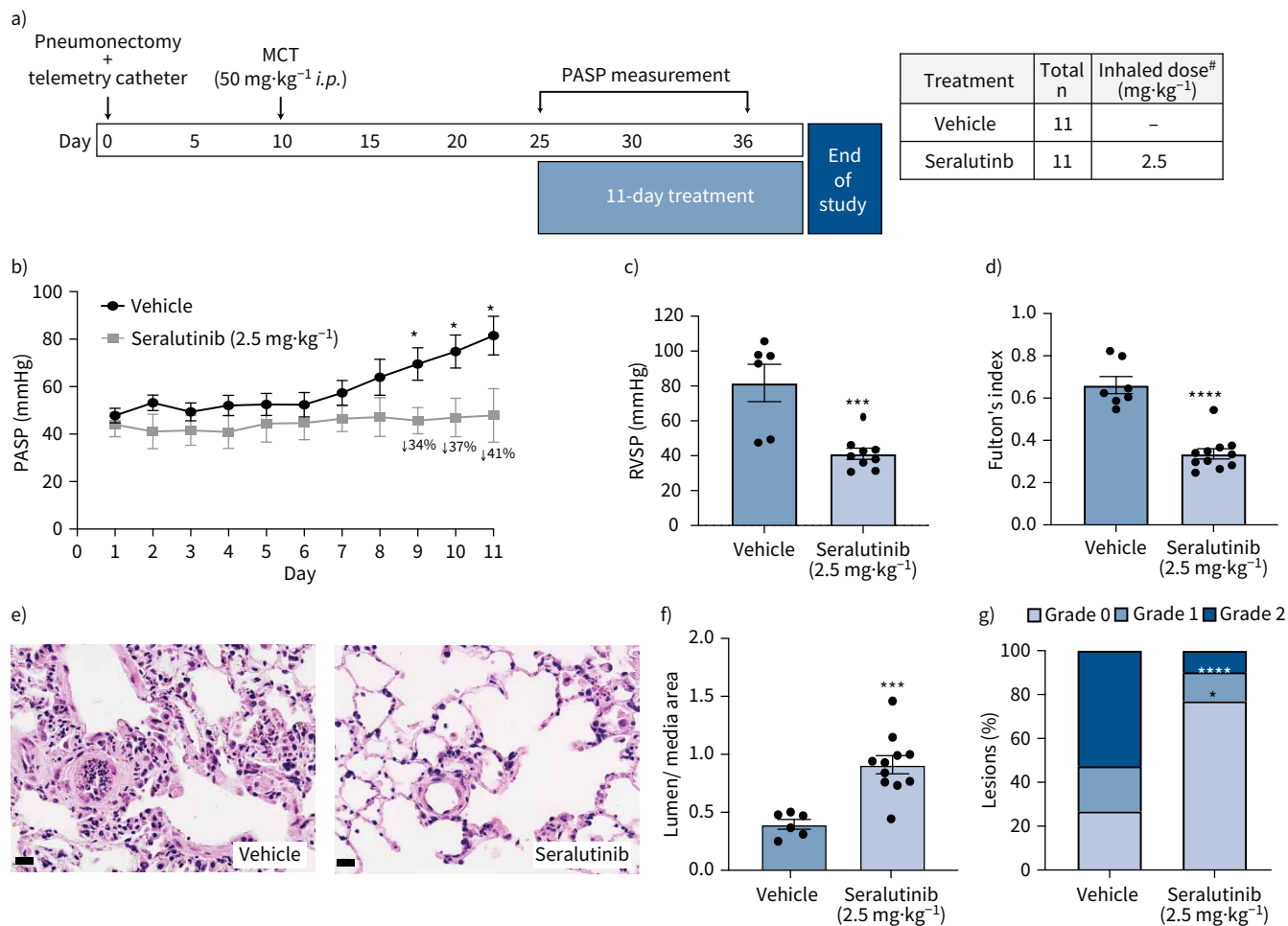
FIGURE 3 Inhaled seralutinib efficacy in SU5416/H model of pulmonary arterial hypertension (PAH). a) SU5416/H model dose-response and telemetry study schema. b) Pulmonary artery systolic pressure (PASP) measured by implanted telemetry device following vehicle and seralutinib (2.5 mg·kg^{-1} twice daily) over the course of treatment. c) Change in right ventricular systolic pressure (RVSP). d) Change in right ventricle hypertrophy by Fulton's index (right ventricular weight)/(weight of left ventricle+interventricular septum). e) Representative photomicrograph of histological changes in lung by haematoxylin and eosin stain. Scale bars: 20 µm. f) Occlusive grading analysis of pulmonary arterioles for seralutinib (4.6 mg·kg^{-1} twice daily) *versus* vehicle; grade 0=no occlusion, grade 1=partial occlusion, grade 2=complete occlusion. g) Lumen/media area change following seralutinib (4.6 mg·kg^{-1} twice daily) *versus* vehicle. h) Representative photomicrographs of immunohistochemistry staining for phosphorylated platelet-derived growth factor receptor β (pPDGFRβ) in seralutinib-treated (4.6 mg·kg^{-1} twice daily) and vehicle-treated animals. Scale bars: 20 µm. Arrow indicates increased pPDGFRβ in an occluded small pulmonary artery. Data represent mean±SEM (for b: vehicle n=3, seralutinib n=9; for c, d, f, g: vehicle n=8–11, seralutinib 2.5 mg·kg^{-1} twice daily n=9, seralutinib 4.6 mg·kg^{-1} twice daily n=5–6). Statistical analysis performed by repeated measures ANOVA for b, ANOVA followed by Dunnett's multiple comparison test for c and d, and unpaired t-test for f and g. Two animals were not used in the telemetry study owing to catheter failures. *s.c.*: subcutaneous. #: twice daily; *: $p < 0.05$; **: $p < 0.005$; ***: $p < 0.001$; ****: $p < 0.0001$, seralutinib *versus* vehicle.

remodelling ($p < 0.001$; figure 4e, f), with fewer grade 1 and 2 lesions (figure 4e, g). A qualitative decrease in perivascular fibrosis was observed in seralutinib-treated lungs compared to vehicle (supplementary figure S1).

Seralutinib significantly improved tidal volume ($p < 0.005$) and decreased respiratory rate ($p < 0.001$) as compared to vehicle (supplementary figure S2a, b). Minute ventilation and airway resistance were similar between seralutinib- and vehicle-treated animals (supplementary figure S2c, d).
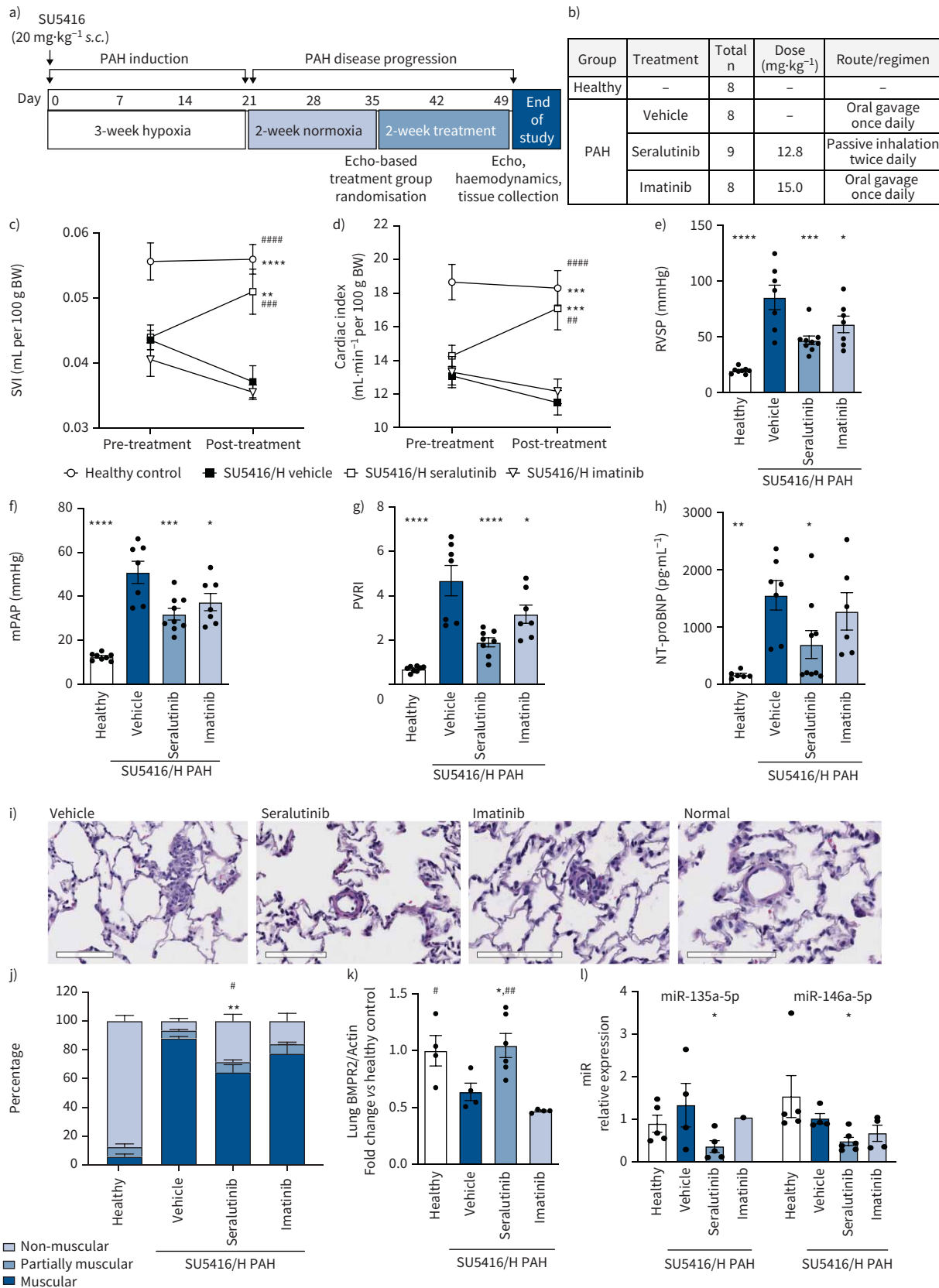
SU5416/H model (Study 3): comparison to imatinib

Seralutinib (12.8 mg·kg^{-1} twice daily), imatinib (15.0 mg·kg^{-1} once daily) or vehicle control (once daily) was administered for 2 weeks following disease induction and a 2-week period of normoxia (figure 5a, b). The imatinib dose selected for the *in vivo* study displayed potent inhibition of PDGFRβ phosphorylation in healthy rats (supplementary figure S3).

FIGURE 4 Inhaled seralutinib efficacy in monocrotaline pneumonectomy (MCTPN) model of pulmonary arterial hypertension (PAH). a) Study schema for MCTPN model and telemetry study. b) Pulmonary artery systolic pressure (PASP) measured by implanted telemetry device for vehicle and seralutinib (2.5 mg·kg^{-1} twice daily) over the course of treatment. c) Change in right ventricular systolic pressure (RVSP). d) Change in right ventricle hypertrophy by Fulton's index (right ventricular weight)/(weight of left ventricle+interventricular septum). e) Representative photomicrographs of histological changes in lung by haematoxylin and eosin stain. Scale bars: 20 μm. f) Lumen/media area following seralutinib (2.5 mg·kg^{-1} twice daily) versus vehicle. g) Occlusive grading analysis of pulmonary arterioles for seralutinib (2.5 mg·kg^{-1} twice daily) versus vehicle; grade 0=no occlusion, grade 1= partial occlusion, grade 2=complete occlusion. Data are presented as mean±SEM (vehicle n=11 for b, n=6–7 for c–f; seralutinib 2.5 mg·kg^{-1} twice daily, n= 9–11). Statistical analysis performed by repeated measures ANOVA for b, and unpaired t-test for c–f. #: twice daily; *: $p<0.05$; ***: $p<0.001$; ****: $p<0.0001$, seralutinib versus vehicle.

At treatment initiation, disease severity was evaluated by echocardiography. Stroke volume index and cardiac index were decreased in diseased animals compared to healthy controls (figure 5c, d). Vehicle-treated PAH rats had elevated RVSP (85.2±11.0 mmHg) and mean pulmonary artery pressure (mPAP) (50.9±5.0 mmHg) compared to healthy controls (RVSP 19.5±1.0 mmHg; mPAP 12.6±0.6 mmHg; $p<0.001$ for both; figure 5e, f). Seralutinib improved haemodynamic parameters, with reductions of 45% in RVSP (46.7±3.9 mmHg) and 37% in mPAP (31.9±2.6 mmHg) compared to vehicle ($p<0.001$; figure 5e f). The decrease in mPAP and improvement in cardiac index resulted in a 60% improvement in PVR index (PVRI) in the seralutinib group ($p<0.0001$; figure 5g). Imatinib reduced RVSP by 28% (61.1±7.4 mmHg) and mPAP by 27% (37.4±3.9 mmHg) ($p<0.05$ versus vehicle; figure 5e, f). Compared to imatinib, seralutinib had a significantly greater effect on stroke volume index and cardiac index (figure 5c, d). The reduction in PVRI from imatinib treatment was ∼37%. Disease induction increased NT-proBNP by nine-fold. Seralutinib decreased NT-proBNP by 55% versus vehicle control ($p<0.05$), while no significant effect was observed with imatinib (figure 5h). Although the effects of seralutinib on these parameters were statistically greater than the effects of imatinib compared to vehicle, there was no statistically significant difference between seralutinib and imatinib with regard to mPAP, RVSP, PVRI or NT-proBNP.

FIGURE 5 Comparison of inhaled seralutinib and oral imatinib efficacy in SU5416/H model of pulmonary arterial hypertension (PAH). a) Study schema for SU5416/H disease induction, progression and b) treatment regimen. Echocardiography (Echo) was performed on day 35 (D35)

(pre-treatment) and D49 (post-treatment) to measure c) change in stroke volume index (SVI) and d) cardiac index (CI) in normoxic control, vehicle, inhaled seralutinib and oral imatinib groups, while e) shows the haemodynamic parameter right ventricular systolic pressure (RVSP) at the end of treatment (D49). f) Mean pulmonary arterial pressure (mPAP), g) pulmonary vascular resistance index (PVRI) (mPAP/cardiac index) and h) change in the peripheral biomarker of N-terminal pro-brain natriuretic protein (NT-proBNP) at the end of treatment (D49). i) Representative photomicrographs of histological changes in lung by hematoxylin and eosin stain. Scale bars: 100 µm. Change in j) muscularisation, k) lung bone morphogenetic protein receptor type 2 (BMPR2) and l) miR-135a-5p and miR-146a-5p. Relative microRNA (miRNA) expression is defined as gene expression fold change relative to the vehicle control group calculated using $2^{-\Delta\Delta Ct}$ values. Data are presented as mean±SEM; healthy n=5–8; vehicle n=4–7; seralutinib n=6–9; imatinib n=4–7; n=3 for all groups for change in muscularisation. Statistical analysis was performed using one-way ANOVA with Dunnett's test for multiple comparisons. Two-way ANOVA with multiple comparison was performed for SVI and cardiac index. One animal was excluded for failure to develop pulmonary hypertension. Statistical analysis of miRNA is described in the supplementary material. s.c.: subcutaneous; BW: body weight. For SVI, CI, RVSP, mPAP, PVRI, NT-proBNP, histological quantification, BMPR2 and miRNA: *: p<0.05; **: p<0.005; ***: p<0.001; ****: p<0.0001 versus vehicle group and #: p<0.05; ##: p<0.005; ###: p<0.001; ####: p<0.0001 versus imatinib.

Haemodynamic improvements were accompanied by a decrease in small pulmonary vessel muscularisation (figure 5i, j). Analysis of haematoxylin and eosin-stained lung sections and α-smooth muscle actin-stained sections demonstrated a decrease in small pulmonary artery muscularisation in the seralutinib group compared to both the vehicle and imatinib-treated groups (figure 5i, j, supplementary figure S4). Seralutinib significantly increased BMPR2, whereas no significant effect on BMPR2 was observed with imatinib (figure 5k). An increase in SMAD1/5 phosphorylation in seralutinib-treated animals was observed, suggesting activation of signalling through BMPR2 (supplementary figure S5).

Effects on biomarkers of inflammation

Seralutinib decreased circulating levels of plasma tumour necrosis factor α (TNF-α) (p<0.001) and increased interleukin (IL)-10 compared to vehicle (p<0.05; figure 6a, b). Imatinib did not significantly alter TNF-α or IL-10 levels. A trend towards decreased PDGF-BB was observed in the seralutinib-treated group (figure 6c). Seralutinib also decreased lung mRNA and protein levels of monocyte chemoattractant protein 1 (MCP-1), a pro-inflammatory cytokine that regulates macrophage recruitment and contributes to MCT-induced pulmonary hypertension [29] (SU5416/H model: p<0.05 compared to vehicle;
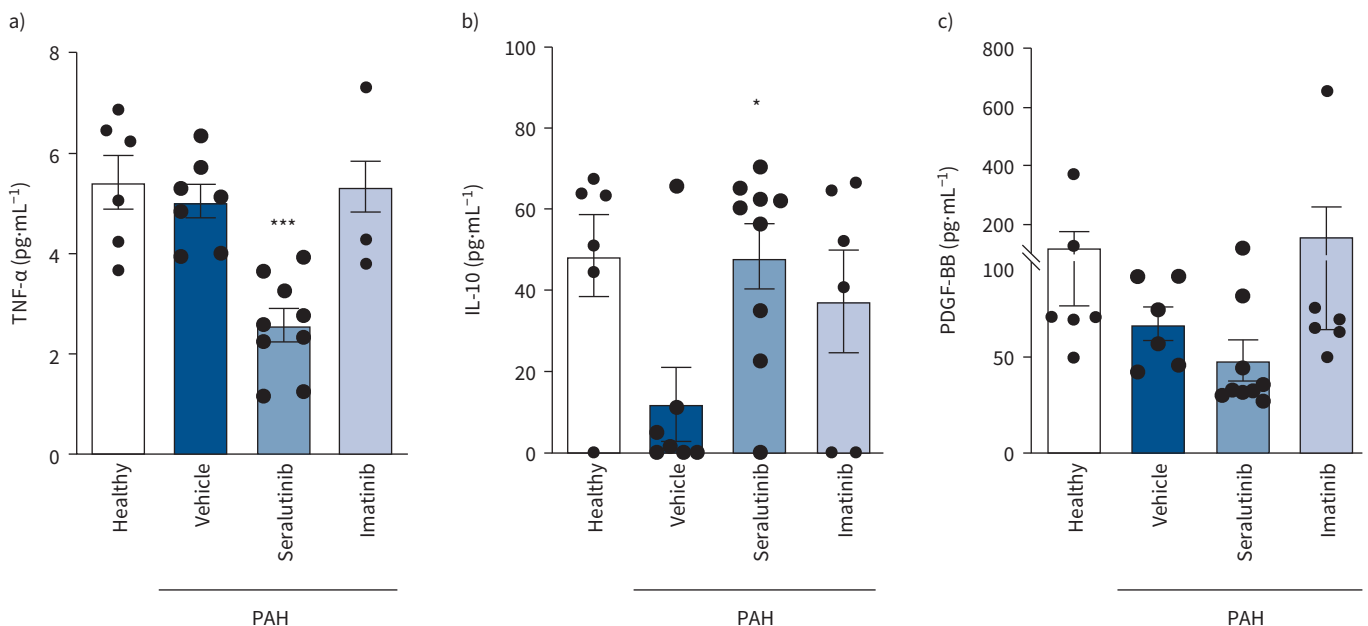
FIGURE 6 Effect of inhaled seralutinib or oral imatinib on the circulating cytokines a) tumour necrosis factor α (TNF-α), b) interleukin 10 (IL-10) and c) platelet-derived growth factor-BB (PDGF-BB) at the end of treatment (day 49) in the SU5416/H pulmonary arterial hypertension (PAH) model. Data are presented as mean±SEM (healthy n=6, vehicle n=6–7, seralutinib n=9, imatinib n=5–6). Statistical analysis performed using one-way ANOVA with Dunnett's multiple comparisons test. *: p<0.05; ***: p<0.001 versus vehicle.

supplementary figure S6b, c). Imatinib did not modulate MCP-1. Seralutinib reduced MCP-1 secretion in a dose-dependent manner in CSF1R$^+$ human macrophages (supplementary figure S6a).

Effect of seralutinib on miRNAs in the lung

Six miRNAs predicted to repress both human and rat BMPR2 were differentially expressed in seralutinib-treated SU5416/H rat lungs relative to vehicle (supplementary table S2). Two of the six miRNAs decreased following treatment with seralutinib compared to vehicle (miR-135a-5p: p=0.01; miR-146a-5p: p=0.02), consistent with the observed increase in BMPR2 protein (figure 5k, l). Four miRNAs were increased by seralutinib, including miR-381-3p, which exhibited the largest expression shift and was significantly higher in seralutinib and imatinib groups relative to vehicle groups.

IHC in iPAH versus control lungs

We evaluated expression of PDGFRα/β, CSF1R and c-KIT proteins in human lung tissue samples to demonstrate relevance of seralutinib targets in iPAH (figure 7). Increases in PDGFRα, PDGFRβ, CSF1R and c-KIT were observed in PAH lung sections compared to controls. IHC in rat lungs from the MCTPN and SU5416/H models showed patterns of PDGFRα/β and CSF1R similar to those seen in human PAH samples (supplementary figures S7 and S8). In both animal models, treatment with seralutinib was associated with decreased signal for PDGFRα/β and CSF1R.
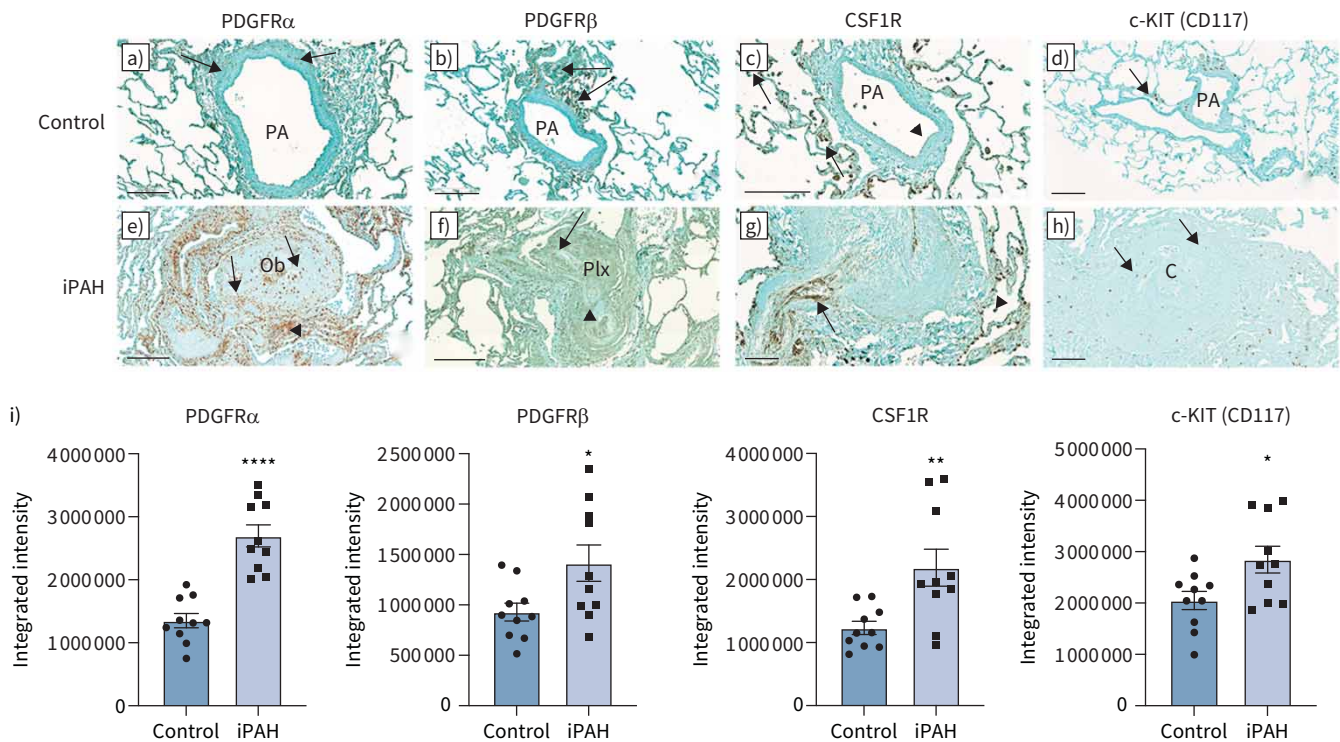
FIGURE 7 Expression of platelet-derived growth factor receptor α (PDGFRα) in a) control and e) idiopathic pulmonary arterial hypertension (iPAH) lung sections, platelet-derived growth factor receptor β (PDGFRβ) in b) control and f) iPAH lung sections, colony-stimulating factor 1 receptor (CSF1R) in c) control and g) iPAH lung sections and mast/stem cell growth factor receptor kit (c-KIT) in d) control and h) iPAH lung sections. PDGFRα is expressed in media smooth muscle cells in normal pulmonary arteries (PAs) in control lungs (arrows) (a), with marked expression in iPAH obliterative lesion (Ob, arrows) and perivascular tissue (arrowhead) (e). PDGFRβ is predominantly expressed in perivascular tissue in control lung (arrows) (b), while a complex plexiform (Plx) pulmonary vascular lesion in iPAH (f) shows intense expression in the intima (arrow) and within the incipient blood vessels and cell clusters (Plx, arrowhead). CSF1R expression is noted in the intima of control PAs (arrowhead), with stronger expression in alveolar macrophages (arrows) (c), while in iPAH lungs, there is marked expression in the intima of obliterative lesion (arrow), with expression in macrophages (arrowhead) (g). Individual c-KIT$^+$ cells are sparsely seen around normal PAs in control lungs (arrow) (d), while iPAH lungs show permeation of concentric vascular lesions (C) with positive cells (arrows) (h). Representative of n=10 control and n=10 iPAH lungs. Scale bars: 100 μm (g), 200 μm (a–e, h), 300 μm (f). i) Quantitative analysis demonstrated a significant increase of integrated intensity for PDGFRα, PDGFRβ, CSF1R and c-KIT in iPAH lung sections compared to controls. *: p<0.05; **: p<0.01; ****: p<0.0001.

Discussion

PDGFR, CSF1R and c-KIT signalling play crucial roles in the pathology and progression of PAH [9–15, 21–26, 30, 31]. Targeting these pathways therefore holds promise as a therapeutic strategy in PAH. Seralutinib is a highly potent PDGFR, CSF1R and c-KIT kinase inhibitor, and is the first and only tyrosine kinase inhibitor intentionally designed as a treatment for PAH. The unique physical properties of seralutinib make it suitable for the inhaled route of administration, potentially optimising therapeutic efficacy while limiting systemic exposure and associated side-effects.

Clinical trials of imatinib in PAH provided proof of concept that targeting PDGFR signalling can affect PAH disease progression [21]. However, further development of imatinib was limited owing to side-effects attributable to relatively high systemic exposure. The clinical experience with imatinib provided impetus and rationale to develop a tyrosine kinase inhibitor targeting pathways relevant to PAH and optimised for delivery directly to the diseased lung by inhalation.

In addition to its optimisation for inhaled delivery, seralutinib displays several other unique features compared to imatinib. For example, only seralutinib inhibited ERK phosphorylation in HLFs. This difference could be important because constitutive activation of ERK1/2 is a driver of proliferation in BMPR2-silenced PAH-derived cells [32]. Seralutinib showed a 13- to 20-fold greater potency at inhibiting proliferation in human PASMCs and HLFs compared to imatinib. Furthermore, seralutinib was more potent than imatinib against CSF1R and c-KIT kinases. A limitation of the current data is the absence of compound profiling in patient-derived cells. PAH-derived PASMCs and HLFs display altered metabolism and functional signalling compared to healthy cells [33, 34]. Future studies using PAH patient cells could provide additional insights into the effects of these compounds.

Two animal models of PAH were used to examine the efficacy of inhaled seralutinib: the SU5416/H model and the MCTPN model. The SU5416/H model reproduces significant features of human PAH, including angio-obliterative lesions and vascular remodelling [35]. The MCTPN model is associated with increased inflammation, fibrosis, increased pulmonary arterial pressure and obstructive neointimal lesions (a feature not observed in the MCT-only model) [36, 37]. While it is recognised that the results of drug studies performed in animal models of PAH do not necessarily translate to human disease, the models we studied replicate key features and different aspects of human PAH. Furthermore, the experiments were designed to demonstrate a therapeutic effect after pulmonary hypertension was established rather than a preventive strategy.

Seralutinib prevented PAH progression in the MCTPN model and reversed pulmonary hypertension in the SU5416/H model in a dose-responsive manner. Haemodynamic improvements were accompanied by reverse pulmonary vascular remodelling, a reduction in NT-proBNP, an increase in pulmonary BMPR2 and an improvement in inflammatory biomarkers. The pathways targeted directly or indirectly by seralutinib stand out as key regulatory nodes in the pathological remodelling associated with PAH (figure 8). In our head-to-head preclinical study, both seralutinib and imatinib decreased mPAP, RVSP, PVRI and NT-proBNP compared to vehicle; however, the effects of seralutinib were more statistically robust. In addition, seralutinib had a greater effect in restoring small pulmonary artery muscularisation towards normal compared to imatinib. Interestingly, BMPR2 was restored to normal levels in the seralutinib-treated group, but not in the imatinib-treated group. Furthermore, while seralutinib decreased MCP-1 (CCL2), imatinib did not. Differences in compound potency, kinase selectivity and downstream signalling profiles as well as target coverage *in vivo* could be contributing to the observed differences between seralutinib and imatinib.

Seralutinib is a more potent PDGFRβ inhibitor than imatinib. Because signalling through PDGFRα and PDGFRβ may mediate different effects important in pathological pulmonary vascular remodelling, potent inhibition of both kinases may lead to improved efficacy *in vivo*. Seralutinib is also a strikingly more potent inhibitor of CSF1R than imatinib, potentially contributing to reduced inflammation and reverse remodelling. In seralutinib-treated animals in the MCTPN study, inhibition of both PDGFR and CSF1R signalling pathways may be contributing to the observed reduction in perivascular fibrosis. Although we cannot rule out that down-modulation of inflammatory markers observed in the current study may be an indirect outcome of seralutinib's reverse remodelling effects, MCP-1 modulation has been directly linked to CSF1R signal transduction in human macrophages [38, 39], and would therefore be indicative of seralutinib target engagement. Future studies to evaluate the potential anti-inflammatory and anti-fibrotic properties of seralutinib would be of interest.

Loss of BMPR2 plays a pivotal role in the pathogenesis of PAH, and crosstalk between PDGFR signalling and BMPR2 expression has been reported [9]. It is known that miRNAs can mediate crosstalk between
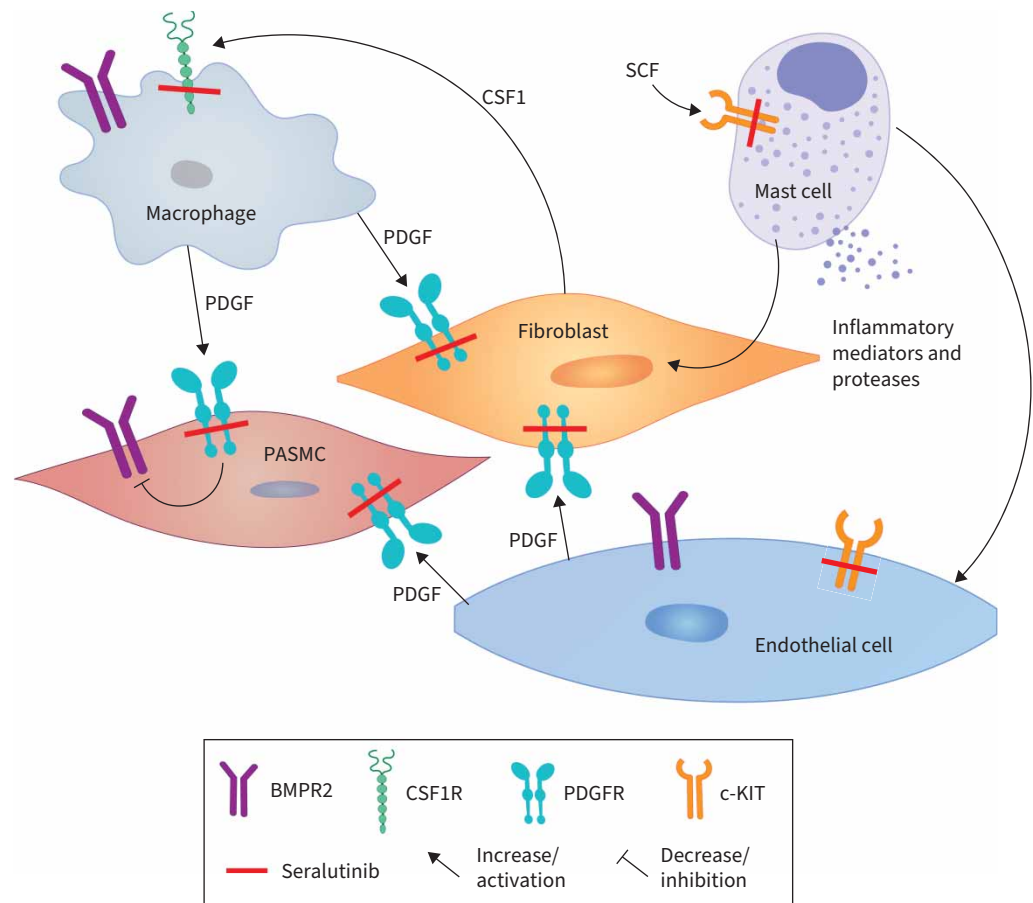
FIGURE 8 Seralutinib inhibits platelet-derived growth factor receptor (PDGFR), colony-stimulating factor 1 receptor (CSF1R) and c-KIT, thereby modulating key signalling pathways involved in pathological remodelling in pulmonary arterial hypertension. Activation of PDGFRs may result in decreased bone morphogenetic protein receptor type 2 (BMPR2) expression. Seralutinib, by inhibiting PDGFR signalling, could increase BMPR2 levels. SCF: stem-cell factor; PDGF: platelet-derived growth factor; PASMC: pulmonary artery smooth muscle cell.

PDGFR signalling and BMPR2, directly by repressing BMPR2 expression or indirectly by repressing other targets that alter BMPR2 [40–42]. We identified six miRNAs predicted to suppress both rat and human BMPR2 that were differentially expressed in SU5416/H rats treated with seralutinib. Of these, miR-135a-5p and miR-146a-5p were decreased in seralutinib-treated lungs, consistent with the observed BMPR2 increase. Of note, miR-135a has previously been implicated in human pulmonary hypertension [42, 43] and linked to BMPR2-specific expression in animal models [41, 44]. For example, in the mouse ovalbumin-urban particulate matter (OVA-PM) model of PAH, treatment with Antago-miR-135a restored BMPR2 to levels observed in healthy lungs [41]. A limitation of our study is that miR-135a-5p expression was only detected in one out of four animals treated with imatinib, which suggests this miRNA may not be the sole contributor to the observed changes in BMPR2 in the seralutinib group (given that BMPR2 in the imatinib group was unchanged). Expression of miR-146a-5p, which decreased with seralutinib in our study, was increased in serum from PAH patients relative to healthy controls, and has been shown to promote proliferation in HPAECs [45]. Although miR-376b is reportedly regulated by PDGF-BB, we did not find a significant regulation of this miRNA in our model [9]. Several additional predicted BMPR2-regulating miRNAs (*i.e.* predicted to reduce BMPR2 protein expression) were elevated following treatment with seralutinib. For example, miR-381-3p was strongly upregulated in the seralutinib and imatinib groups compared to vehicle. This miRNA is predicted to weakly repress BMPR2 but also functions as a tumour suppressor, blocking proliferation in cancer cell lines [46]. Furthermore, increased miR-381-3p has been shown to repress TGF-β and inhibit proliferation of human bronchial smooth muscle cells [47]. The net effect on BMPR2 expression of these miRNAs as an ensemble has not been characterised and is difficult to predict. Future studies could shed light on the contribution of each miRNA to seralutinib's mechanism of action. Regardless of mechanism, the increase in BMPR2 following

seralutinib treatment could lead to synergistic effects in combination with therapeutic approaches specifically targeting the activin/TGF-β pathway.

Seralutinib is also a potent c-KIT inhibitor and decreased SCF-induced autophosphorylation of KIT in HPAECs. Hypoxia has been shown to increase c-KIT expression on pulmonary endothelial cells, enhancing the angiogenic response to SCF and contributing to pulmonary vascular pathology in the SU5416/H rat model [26]. Infiltration of c-KIT$^+$ cells (endothelial progenitor cells and mast cells) was also reported in pulmonary arterial plexiform lesions in PAH lungs [8, 23, 27, 48]. Lung-targeted delivery of seralutinib may mitigate risks associated with systemic c-KIT inhibition by limiting inhibition to the disease site.

Quantitative IHC demonstrated increased integrated intensity of PDGFRα, PDGFRβ, CSF1R and c-KIT in human PAH lungs compared to controls. Our findings are consistent with previous reports of increased expression of PDGFRα, PDGFRβ and c-KIT in human PAH lungs [11, 23]. To our knowledge, this is the first report of increased CSF1R expression in human PAH. These findings support the relevance of targeting CSF1R in addition to PDGFRs and c-KIT in PAH. IHC of PDGFRα/β and CSF1R in both the rat MCTPN and SU5416/H models showed patterns similar to those seen in human PAH.

In conclusion, seralutinib delivered as an inhaled dry powder was effective in two preclinical models of PAH. Because these animal models of PAH replicate different features of the human disease, the fact that seralutinib demonstrated robust efficacy in both models increases the likelihood of seralutinib's efficacy as a treatment in human PAH. The improvement in BMPR2 levels observed with seralutinib is consistent with the reverse remodelling of small pulmonary arteries in PAH. Current standard-of-care treatments in PAH function primarily as vasodilators, with limited effects on neointimal proliferation and pulmonary vascular remodelling. Our studies indicate that seralutinib has a direct ameliorative impact on pulmonary vascular remodelling that results in improved cardiopulmonary haemodynamic parameters. The design of these studies ensured that seralutinib was initiated under fully established disease conditions, thus demonstrating the potential for efficacy in a therapeutic setting. Observed reverse remodelling of the small pulmonary arteries and restoration of lung BMPR2 expression in the rat PAH models suggest that seralutinib may have an impact on underlying causes of PAH. Seralutinib is currently in clinical development for patients with PAH (NCT04456998).

References

1   Cool CD, Kuebler WM, Bogaard HJ, *et al.* The hallmarks of severe pulmonary arterial hypertension: the cancer hypothesis–ten years later. *Am J Physiol Lung Cell Mol Physiol* 2020; 318: L1115–L1130.

2   El Chami H, Hassoun PM. Inflammatory mechanisms in the pathogenesis of pulmonary arterial hypertension. *Compr Physiol* 2011; 1: 1929–1941.

3   Humbert M, Hoeper MM. Severe pulmonary arterial hypertension: a forme fruste of cancer? *Am J Respir Crit Care Med* 2008; 178: 551–552.

4   Pullamsetti SS, Savai R, Seeger W, *et al.* Translational advances in the field of pulmonary hypertension. From cancer biology to new pulmonary arterial hypertension therapeutics. Targeting cell growth and proliferation signaling hubs. *Am J Respir Crit Care Med* 2017; 195: 425–437.

5   Rai PR, Cool CD, King JA, *et al.* The cancer paradigm of severe pulmonary arterial hypertension. *Am J Respir Crit Care Med* 2008; 178: 558–564.

6   Stacher E, Graham BB, Hunt JM, *et al.* Modern age pathology of pulmonary arterial hypertension. *Am J Respir Crit Care Med* 2012; 186: 261–272.

7   Boucherat O, Vitry G, Trinh I, *et al.* The cancer theory of pulmonary arterial hypertension. *Pulm Circ* 2017; 7: 285–299.

8   Jonigk D, Golpon H, Bockmeyer CL, *et al.* Plexiform lesions in pulmonary arterial hypertension composition, architecture, and microenvironment. *Am J Pathol* 2011; 179: 167–179.

9   Chen J, Cui X, Qian Z, *et al.* Multi-omics analysis reveals regulators of the response to PDGF-BB treatment in pulmonary artery smooth muscle cells. *BMC Genomics* 2016; 17: 781.

10   Grimminger F, Schermuly RT. PDGF receptor and its antagonists: role in treatment of PAH. *Adv Exp Med Biol* 2010; 661: 435–446.

11   Perros F, Montani D, Dorfmuller P, *et al.* Platelet-derived growth factor expression and function in idiopathic pulmonary arterial hypertension. *Am J Respir Crit Care Med* 2008; 178: 81–88.

12   Schermuly RT, Dony E, Ghofrani HA, *et al.* Reversal of experimental pulmonary hypertension by PDGF inhibition. *J Clin Invest* 2005; 115: 2811–2821.

13   Stavri GT, Hong Y, Zachary IC, *et al.* Hypoxia and platelet-derived growth factor-BB synergistically upregulate the expression of vascular endothelial growth factor in vascular smooth muscle cells. *FEBS Lett* 1995; 358: 311–315.

14   Ten Freyhaus H, Berghausen EM, Janssen W, *et al.* Genetic ablation of PDGF-dependent signaling pathways abolishes vascular remodeling and experimental pulmonary hypertension. *Arterioscler Thromb Vasc Biol* 2015; 35: 1236–1245.

15   Saygin D, Tabib T, Bittar HET, *et al.* Transcriptional profiling of lung cell populations in idiopathic pulmonary arterial hypertension. *Pulm Circ* 2020; 10: 1–15.

16   Wu E, Palmer N, Tian Z, *et al.* Comprehensive dissection of PDGF-PDGFR signaling pathways in PDGFR genetically defined cells. *PLoS One* 2008; 3: e3794.

17   Kudryashova TV, Shen Y, Pena A, *et al.* Inhibitory antibodies against activin A and TGF-β reduce self-supported, but not soluble factors-induced growth of human pulmonary arterial vascular smooth muscle cells in pulmonary arterial hypertension. *Int J Mol Sci* 2018; 19: 2957.

18   Porsch H, Mehic M, Olofsson B, *et al.* Platelet-derived growth factor β-receptor, transforming growth factor β type I receptor, and CD44 protein modulate each other's signaling and stability. *J Biol Chem* 2014; 289: 19747–19757.

19   Atkinson C, Stewart S, Upton PD, *et al.* Primary pulmonary hypertension is associated with reduced pulmonary vascular expression of type II bone morphogenetic protein receptor. *Circulation* 2002; 105: 1672–1678.

20   Ghofrani HA, Morrell NW, Hoeper MM, *et al.* Imatinib in pulmonary arterial hypertension patients with inadequate response to established therapy. *Am J Respir Crit Care Med* 2010; 182: 1171–1177.

21   Hoeper MM, Barst RJ, Bourge RC, *et al.* Imatinib mesylate as add-on therapy for pulmonary arterial hypertension: results of the randomized IMPRES study. *Circulation* 2013; 127: 1128–1138.

22   Stanley ER, Chitu V. CSF-1 receptor signaling in myeloid cells. *Cold Spring Harb Perspect Biol* 2014; 6.

23   Montani D, Perros F, Gambaryan N, *et al.* C-kit-positive cells accumulate in remodeled vessels of idiopathic pulmonary arterial hypertension. *Am J Respir Crit Care Med* 2011; 184: 116–123.

24   Abid S, Marcos E, Parpaleix A, *et al.* CCR2/CCR5-mediated macrophage-smooth muscle cell crosstalk in pulmonary hypertension. *Eur Respir J* 2019; 54: 1802308.

25   Sheikh AQ, Saddouk FZ, Ntokou A, *et al.* Cell autonomous and non-cell autonomous regulation of SMC progenitors in pulmonary hypertension. *Cell Rep* 2018; 23: 1152–1165.

26   Farkas D, Kraskauskas D, Drake JI, *et al.* CXCR4 inhibition ameliorates severe obliterative pulmonary hypertension and accumulation of C-kit$^+$ cells in rats. *PLoS One* 2014; 9: e89810.

27   Toshner M, Voswinckel R, Southwood M, *et al.* Evidence of dysfunction of endothelial progenitors in pulmonary arterial hypertension. *Am J Respir Crit Care Med* 2009; 180: 780–787.

28   Joshi N, Watanabe S, Verma R, et al. A spatially restricted fibrotic niche in pulmonary fibrosis is sustained by M-CSF/M-CSFR signalling in monocyte-derived alveolar macrophages. Eur Respir J 2020; 55: 1900646.

29   Ikeda Y, Yonemitsu Y, Kataoka C, et al. Anti-monocyte chemoattractant protein-1 gene therapy attenuates pulmonary hypertension in rats. Am J Physiol Heart Circ Physiol 2002; 283: H2021–H2028.

30   Savai R, Pullamsetti SS, Kolbe J, et al. Immune and inflammatory cell involvement in the pathology of idiopathic pulmonary arterial hypertension. Am J Respir Crit Care Med 2012; 186: 897–908.

31   Talati M, West J, Zaynagetdinov R, et al. BMP pathway regulation of and by macrophages. PLoS One 2014; 9: e94119.

32   Awad KS, Elinoff JM, Wang S, et al. Raf/ERK drives the proliferative and invasive phenotype of BMPR2-silenced pulmonary artery endothelial cells. Am J Physiol Lung Cell Mol Physiol 2016; 310: L187–L201.

33   Wu K, Tang H, Lin R, et al. Endothelial platelet-derived growth factor-mediated activation of smooth muscle platelet-derived growth factor receptors in pulmonary arterial hypertension. Pulm Circ 2020; 10: 2045894020948470.

34   Barnes JW, Tian L, Heresi GA, et al. O-linked β-N-acetylglucosamine transferase directs cell proliferation in idiopathic pulmonary arterial hypertension. Circulation 2015; 131: 1260–1268.

35   Taraseviciene-Stewart L, Kasahara Y, Alger L, et al. Inhibition of the VEGF receptor 2 combined with chronic hypoxia causes cell death-dependent pulmonary endothelial cell proliferation and severe pulmonary hypertension. FASEB J 2001; 15: 427–438.

36   Okada K, Tanaka Y, Bernstein M, et al. Pulmonary hemodynamics modify the rat pulmonary artery response to injury. A neointimal model of pulmonary hypertension. Am J Pathol 1997; 151: 1019–1025.

37   White RJ, Meoli DF, Swarthout RF, et al. Plexiform-like lesions and increased tissue factor expression in a rat model of severe pulmonary arterial hypertension. Am J Physiol Lung Cell Mol Physiol 2007; 293: L583–L590.

38   Bellamri N, Morzadec C, Joannes A, et al. Alteration of human macrophage phenotypes by the anti-fibrotic drug nintedanib. Int Immunopharmacol 2019; 72: 112–123.

39   Wlodarczyk A, Benmamar-Badel A, Cedile O, et al. CSF1R stimulation promotes increased neuroprotection by CD11c+ microglia in EAE. Front Cell Neurosci 2018; 12: 523.

40   Brock M, Trenkmann M, Gay RE, et al. Interleukin-6 modulates the expression of the bone morphogenic protein receptor type II through a novel STAT3-microRNA cluster 17/92 pathway. Circ Res 2009; 104: 1184–1191.

41   Lee HW, Park SH. Elevated microRNA-135a is associated with pulmonary arterial hypertension in experimental mouse model. Oncotarget 2017; 8: 35609–35618.

42   Santos-Ferreira CA, Abreu MT, Marques CI, et al. Micro-RNA analysis in pulmonary arterial hypertension: current knowledge and challenges. JACC Basic Transl Sci 2020; 5: 1149–1162.

43   Parikh VN, Jin RC, Rabello S, et al. MicroRNA-21 integrates pathogenic signaling to control pulmonary hypertension: results of a network bioinformatics approach. Circulation 2012; 125: 1520–1532.

44   Liu HM, Jia Y, Zhang YX, et al. Dysregulation of miR-135a-5p promotes the development of rat pulmonary arterial hypertension in vivo and in vitro. Acta Pharmacol Sin 2019; 40: 477–485.

45   Zhang W, Qi Y, Wu B. MicroRNA-146-5p promotes pulmonary artery endothelial cell proliferation under hypoxic conditions through regulating USP3. Dis Markers 2021; 2021: 3668422.

46   Yu YZ, Mu Q, Ren Q, et al. miR-381-3p suppresses breast cancer progression by inhibition of epithelial-mesenchymal transition. World J Surg Oncol 2021; 19: 230.

47   Bai SY, Li ML, Ren Y, et al. HDAC8-inhibitor PCI-34051-induced exosomes inhibit human bronchial smooth muscle cell proliferation via miR-381-3p mediated TGFB3. Pulm Pharmacol Ther 2021; 71: 102096.

48   Stearman RS, Bui QM, Speyer G, et al. Systems analysis of the human pulmonary arterial hypertension lung transcriptome. Am J Respir Cell Mol Biol 2019; 60: 637–649.